Ordered Structures in Proton Conducting Membranes from Supramolecular Liquid Crystal Polymers

Hayley A. Every,* Eduardo Mendes,* and Stephen J. Picken

Polymer Materials and Engineering, Delft University of Technology, Julianalaan 136, 2628BL Delft, The Netherlands and Dutch Polymer Institute (DPI), P.O. Box 902, 5600 AX Eindhoven, The Netherlands

Received: July 12, 2006; In Final Form: September 14, 2006

Highly sulfonated forms of poly(*p*-phenylene terephthalamide) (PPTA) have been prepared in three different molecular configurations; sulfonated diamine form (S-PPTA), sulfonated terephthalic acid form (S-invert-PPTA), and the bi-sulfonated form (S^2-PPTA). All three polymers are water soluble to a certain degree and films were cast from solution for S-PPTA and S-invert-PPTA. S-PPTA films absorb less water than S-invert-PPTA (under controlled humidity conditions) and consequently, the conductivity for this polymer is also slightly lower. Although the conductivities are comparable to Nafion (of the order of 10^{-2} to 10^{-1} Scm^{-1}), proton mobility is more restricted. X-ray diffraction showed that the rigid molecules are aligned in opposite directions for the two polymer films, being homeotropic in S-PPTA films and planar for S-invert-PPTA. SEM analysis demonstrated layering in the same direction as the alignment of the polymer chains. The variation in the polymer alignment is most likely the result of the differences in the solution properties and the film forming process. It is possible, however, that this alignment could be exploited to enhance proton transport and thus these films are of interest for fuel cell membranes.

1. Introduction

In the development of polymer electrolytes for fuel cells, the proton conductivity is not the only consideration; mechanical integrity, as well as thermal and chemical stability, are also of importance. With this in mind, sulfonated high performance polymers, such as polyimides, poly(ether ether ketone)s, poly(ether sulfone)s, and polyaramides, have been investigated as new membrane materials.

Several groups have reported the synthesis and characterization of sulfonated polyimides.[1−7] The membrane properties are sensitive to the degree and distribution of sulfonated groups (block size) and the chemical structure of the polymer, i.e., the incoporation of either a phthalic or naphthalic group within the polymer backbone. Maximum conductivities were observed for higher degrees of sulfonation[7] and shorter block lengths.[3] A strong anisotropy in the transport properties was observed, with both the conductivity and ionic diffusion coefficients exhibiting higher values within the plane of the film than through the film.[5] SAXS measurements of these membranes also revealed structural anisotropy through the thickness of the film, while the in-plane diffraction was isotropic. Despite their competitive properties, the applicability of these materials as fuel cell membranes is likely to be hindered by their long-term stability; the polymers are susceptible to hydrolysis, with the phthalic form being more sensitive than the naphthalic polymer.[4,7]

Sulfonated poly(ether ether ketones) (S−PEEK) have also been studied, where the diether substituted ring in the polymer is post-sulfonated in the presence of sulfuric acid.[8,9] The degree of sulfonation is dependent on the acid concentration as well as the reaction time and temperature.[8,9] The conductivity increases with increasing degree of sulfonation,[9−11] however, it is only at the highest levels of sulfonation that PEEK starts to compete with Nafion.[10,12] Sulfonated PEEK absorbs a substantial amount of water (up to 30 water molecules per sulfonic acid group), and furthermore, treating the polymer in boiling water prior to testing results in substantially higher conductivity values.[10] The thermal stability of post-sulfonated polymers is always inferior to pre-polymerization sulfonation.[10] However, several groups have successfully prepared sulfonated PEEK from sulfonated monomers,[13−15] which should help with the long-term stability.

McGrath and co-workers[16−21] have developed a series of random copolymers based on poly(arylene ether sulfones). The degree of sulfonation can be controlled during the reaction[16,17] and ranges from 0 to 60 mol %. Conductivities are highest for the most sulfonated polymers (of the order of 10^{-1} Scm^{-1}). However, the mechanical stability deteriorates in the presence of water for the polymers with sulfonation levels above 50 mol %. The properties seem to be largely dependent on the amount of water present within the membrane; the pretreatment of the polymer has been shown to influence the domain morphology and thus the water uptake.[18,19] Upon incorporating these membranes into both hydrogen and direct methanol fuel cells,[22] the performance is highly competitive with respect to Nafion. This is particularly true in the case of direct methanol fuel cells, where Nafion suffers from extensive methanol crossover. Therefore, these materials are a particularly attractive alternative fuel cell membrane.

Meier-Haack and co-workers[23−25] have looked at derivatives of sulfonated PPTA for fuel cell applications. The properties of a fully sulfonated PPTA were compared to copolymers based on sulfonated PPTA and 4,4-oxyanaline.[23,24] For the copolymers, the properties of the polymer were dependent on the block length, with longer blocks resulting in more phase separation and greater water absorption. The conductivity of these polymers at 100% relative humidity was of the order of $10^{-3}Scm^{-1}$. Long-

* Corresponding authors. E-mail: H.A.Every@tudelft.nl; E.Mendes@tudelft.nl. Telephone: +31 15 278 4365 (H. E.); +31 15 278 2623 (E. M.). Fax: +31 15 278 7415 (H. E. and E. M.).

10.1021/jp064398i CCC: $33.50
Published on Web 10/24/2006

SCHEME 1. Chemical Structures of (A) S−PPTA, (B) S-invert-PPTA, and (C) S²-PPTA

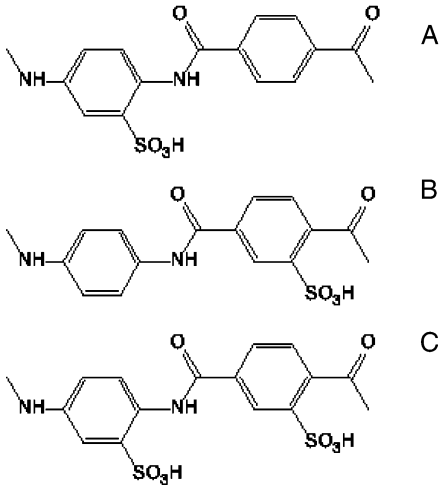

term stability of these membranes was assessed in water or hydrochloric acid solutions at elevated temperatures and pressures.[25] Over a period of 70 h, a 25% reduction in viscosity was observed for sulfonated PPTA, possibly the result of hydrolytic cleavage at the amide bond. The degradation process was accelerated by the presence of the hydrochloric acid. Although no desulfonation was detected, these results still raise questions concerning the durability of these polymers.

For each of the above-mentioned polymer systems, the morphology of the membrane has not been specifically tailored to promote proton conduction but, in most cases, has evolved from any phase separation experienced by block copolymers. Viale and co-workers,[26−29] however, demonstrated that it is possible to control the alignment of supramolecular aggregates of sulfonated PPTA in liquid crystalline water solutions by means of shearing or exposure to magnetic fields. Furthermore, the solution properties are strongly dependent on the location of the sulfonic acid group on the polymer chain. Two monofunctional polymers were prepared; S-PPTA with the sulfonic acid group attached to the diamine monomer (Scheme 1a)[30] and S-invert-PPTA where the sulfonic acid group is located on the terephthalic acid monomer (Scheme 1b).[26,31] Based on the principles of these synthesis procedures, a bifunctional polymer was also prepared, with the sulfonic acid functionality attached to both monomer groups (S^2-PPTA, Scheme 1c).[32] S-PPTA forms a gel in water, even at concentrations as low as 1 wt %.[30] Below ~2 wt %, the gels are isotropic, while above this concentration, birefringence was observed, indicating of the formation of supramolecular aggregates.[29] Water solutions of S-invert-PPTA, however, are free-flowing liquids up to the solubility limit (10 wt % for the acid form).[31] Isotropic behavior was observed below 1 wt % with fully nematic solutions seen above 3 wt %. Evidence of the nematic phase at such low concentrations implies the formation of supramolecular aggregates.[31] Upon heating, a transition from a nematic to isotropic phase is observed at approximately 70 °C, indicating an instability in the supramolecular phase above these temperatures. The third polymer, S^2-PPTA, on the degree of sulfonation alone would be an excellent candidate for fuel cell membranes. The fact, however, that it is extremely soluble in water, forming solutions up to 60 wt %,[32] makes it difficult to cast into films, thus precluding the use of this material for membranes. In this sample, nematic textures were also observed for solutions above 40 wt %. The phase behavior was also found to be temperature dependent, with the isotropic−nematic transition shifting to higher S^2-PPTA weight fractions as the temperature increased. The shift in onset of the nematic phase to higher polymer fractions suggests the formation of a molecular liquid crystalline phase.[32] The aggregate dimensions for S-PPTA and S-invert-PPTA were assessed using scattering techniques, the results of which are shown in Table 1.[26−28] S-PPTA forms slightly larger aggregates compared to S-invert-PPTA. S^2-PPTA, however, exhibits little or no aggregation, which is consistent with a molecular solution.[32] In summary, the differences in the solubility and solution behavior for these sulfonated PPTA polymers appears to be related to the interactions experienced by the polymer and/or aggregates.

TABLE 1: Sulfonated PPTA Polymer Molecular Weights and Typical Aggregate Dimensions for ±1 wt % Solutions as Determined by X-ray and Neutron Scattering[26−28]

polymer	MW/gmol^{-1}	diameter/Å	length/Å
S-PPTA	18 000	30	12 000
S-invert-PPTA	10 000	22	8700

The research on these materials, conducted by Viale et al., thus far was entirely in the solution phase. It is hypothesized that the alignment observed in the solution phase can also be maintained upon film formation. In this work, films have been prepared from the sulfonated PPTA polymers and the proton transport properties investigated. The results are discussed in relation to the aggregate interactions in solution and the corresponding alignment of the polymer chains within the film.

2. Experimental Section

2.1. Sample Preparation. The polymers were synthesized as reported elsewhere.[30−32] Films of each polymer were prepared from 1 wt % solutions of the polymers in water. The solutions were vigorously boiled for 10 min to ensure complete solubilization. The solutions were cooled (during which the aggregates are formed) and then cast onto a Teflon plate. The samples were left to dry for 24 h, followed by further drying under vacuum at 40 °C for another 24 h. S-PPTA and S-invert-PPTA form nice, albeit brittle, films: S^2-PPTA is extremely hygroscopic making it difficult to produce thin films.

2.2. Ion Exchange Capacity. The ion exchange capacity was determined via titration with 0.5M NaOH. Given that the polymers are soluble in water, the titration was performed directly using the polymer solutions. Phenolphthalein was used as the endpoint indicator.

2.3. Film Characterization. Water uptake was determined by placing a small amount of each polymer in a controlled humidity environment. Samples were exposed to relative humidities of 40, 60, 80, and 100%, as determined by lithium chloride solutions of differing concentrations.[33] Wet and dry weights were recorded and the level of hydration, λ, determined based on the ion exchange capacities.

A Phillips Scanning Electron Microscope (XL 20) with 15kV electron source was used to investigate the film structure.

In-plane proton conductivities were measured with a Novacontrol Alpha Analyzer dielectric response analyzer. A standard windowpane system with indium electrodes was employed, allowing the samples to be exposed to an atmosphere of 100% relative humidity (vapor equilibrated). The measurements were performed over a temperature range of 26−90 °C and a frequency range of 1 MHz to 0.1 Hz.

Wide-angle X-ray scattering experiments were performed using a Bruker-Nonius D8-Discover setup equipped with 2D detector. The sample−detector (S−D) distance was set at 6 cm,

TABLE 2: Theoretical and Experimental Ion Exchange Capacities for Sulfonated PPTA polymers

polymer	theoretical IEC/meqg^{-1}	experimental IEC/meqg^{-1}
S-PPTA	3.14	2.7 ± 0.1
S-invert-PPTA	3.14	3.6 ± 0.1
S^2-PPTA	5.02	4.9 ± 0.1
Nafion 117	0.91	-

and the incident beam wavelength was 1.54 Å (Cu−Kα). Measurements were taken perpendicular to and in the plane of the films.

3. Results and Discussion

The three polymers described in this paper differ only in the placement of the sulfonic acid group(s) (see Scheme 1). For S-PPTA, the sulfonic acid is positioned on the diamine monomer of the repeating unit; in the case of S-invert-PPTA, it is located on the terephthalic acid moiety. S^2-PPTA has two sulfonic acid groups, one on each monomer unit. An indication of the degree of sulfonation is given by the ion exchange capacity (IEC), which is defined as the number of ionic sites for a given molecular weight and is reported in milli-equivalents per gram. The experimentally obtained IEC values are compared to the theoretical values for all three polymers in Table 2. For S^2-PPTA, the values are within experimental error. The experimental value for S-PPTA is slightly lower than the predicted; for S-invert-PPTA, it is slightly higher. Although the differences in IEC values for S-PPTA and S-invert-PPTA are unexpected, the results are consistent with previously reported TGA data that indicate a smaller mass loss around 280 °C (corresponding to the sulfonic acid group) for S-PPTA.[30,31] Nafion 117 is the current standard fuel cell membrane material and is, therefore, often used as a basis for comparison for new membrane materials. The IEC values for the sulfonated PPTA polymers are three to five times higher than that of Nafion 117, indicating a greater density of sulfonic acid groups for these sulfonated PPTA polymers.

To examine the applicability of these polymers as fuel cell membranes, films were prepared. S-PPTA and S-invert-PPTA form good films; S^2-PPTA is too hygroscopic thus making film formation very difficult. Consequently, the discussion of the film properties will be limited to S-PPTA and S-invert-PPTA. Water uptake measurements were conducted at room temperature for the films exposed to different relative humidities. The water uptake values are the difference between the wet and dry weights. In Figure 1, the number of water molecules per sulfonic group as a function of the water activity (relative humidity) is presented for each polymer; the data for Nafion 117 has been reproduced from ref 34 for comparison. Despite the similarities between these two PPTA polymers, the water uptake is different for each, with S-PPTA absorbing less water that S-invert-PPTA over the entire range of humidities studied. The ability to absorb water must be related to the positioning of the sulfonic acid group and the interactions it experiences. It was previously proposed that the sulfonic acid group in S-PPTA is involved in *intra*molecular interactions that would, therefore, limit accessibility for water absorption, thus reducing the overall water content.[31,35] It is also possible, and more plausible in the bulk (as in this case), that *inter*molecular or *inter*aggregate interactions also play a role. In any case, such interactions do not appear to be present for S-invert-PPTA as supported by FTIR data[28] and consequently a stronger interaction between the sulfonic acid group and water is possible.

For relative humidities less than 100%, the water content for the sulfonated PPTA polymers is slightly lower than that of Nafion. At 100% relative humidity, the water uptake of both sulfonated PPTA polymers surpasses that of Nafion, with water contents of approximately 100 and 165 molecules per sulfonic acid group for S-PPTA and S-invert-PPTA, respectively. It should be noted that under such conditions, the membrane is no longer mechanically stable, making the films very difficult to handle. Furthermore, at these high water contents, considerable swelling (∼100%) was also observed.

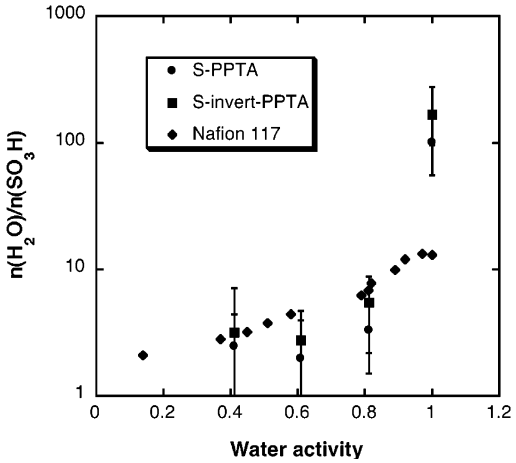

Figure 1. Water uptake (given as the ratio of water molecules per sulfonic acid group) as a function of water activity (relative humidity) for S-PPTA and S-invert-PPTA. The Nafion data, reproduced from ref 34, have been shown for comparison.

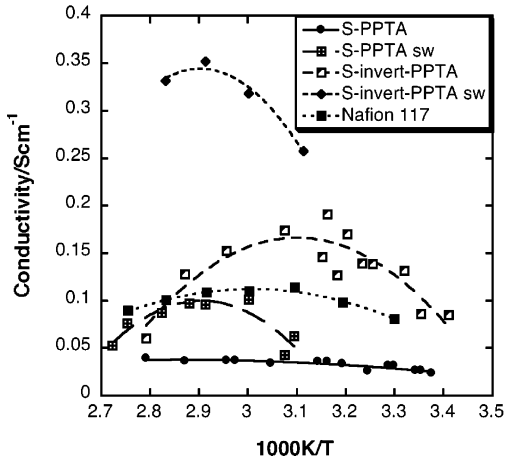

Figure 2. Conductivity measurements as a function of reciprocal temperature for S-PPTA and S-invert-PPTA. Data are shown for the initial measurements and also after the polymer is swollen (indicated by sw). The Nafion data, reproduced from ref 36, have been shown for comparison.

Conductivity measurements in the plane of the film were measured at 100% relative humidity (vapor equilibrated) and as a function of temperature. The results for the two PPTA polymers are shown in Figure 2; the data for Nafion has been reproduced from ref 36 for comparison. S-PPTA has the lowest conductivity of all three polymers, while S-invert-PPTA actually exceeds the conductivity of Nafion over most of the temperature range studied. S-PPTA shows a small but steady increase in conductivity with increasing temperature while both S-invert-PPTA and Nafion exhibit a maximum in conductivity at approximately 45 and 60 °C, respectively. Above these temperatures, evaporation takes place and the conductivity, therefore, decreases. With the PPTA polymers, a hysteresis is observed resulting in higher conductivities upon cooling (also seen in Figure 2). As reported earlier, these polymers have a

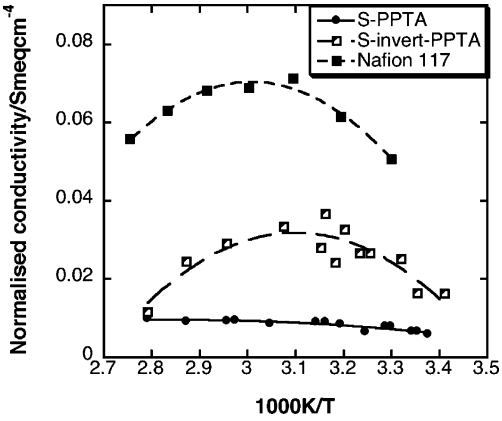

Figure 3. Normalized conductivity with respect to the number of charge carriers per unit volume. Data are again shown for the sulfonated PPTA polymers in the nonswollen state and Nafion 117.

tendency to swell at high relative humidities, a phenomenon that is likely to be exacerbated at higher temperatures. The swelling of the polymer is accompanied by increased water absorption, thus accounting for the enhancement in conductivity that is observed after heating the sample.

In comparing the conductivities of the sulfonated PPTA polymers to Nafion, the values are very similar, yet the number of charge carriers is considerably higher for the sulfonated PPTA polymers (see Table 2). It, therefore, appears that the structure of the polymer must influence the ability to transport protons. To examine the difference in proton mobility, the conductivity values were divided by the ion exchange capacity and polymer density (densities of PPTA and Nafion are 1.45 and 1.75gcm^{-1}, respectively[37,38]); the results of which are shown in Figure 3. This normalizes the data with respect to the number of charge carriers per unit volume and was performed for both the PPTA polymers (in the nonswollen state) and for Nafion. The results clearly show that the proton mobility is higher in Nafion than the two PPTA polymers over the entire temperature range. From this, it seems that although the number of charge carriers is greater in the case of the PPTA polymers, the structure of the film limits the mobility and thus the overall conductivity. In reaching this conclusion, it is assumed that the proton dissociation is the same in both systems, when in actual fact, it may be influenced by the neighboring chemical structure and aggregation. However, density functional theory (DFT) calculations of the lithium binding energies for model compounds based on sulfonated PPTA polymers and Nafion gave almost the same values.[35] By analogy, the proton dissociation is expected to be similar in both systems and thus, the normalized conductivity data is indeed an indication of the proton mobility within these polymers.

The difference in conductivity between the two PPTA polymers is partly related to the proton availability. Despite the fact that the polymers are chemically identical, the experimental ion exchange capacity is lower for S-PPTA. Furthermore, the sulfonic acid groups in S-PPTA are thought to be involved in intermolecular or inter-aggregate interactions since in low concentration aqueous solutions, they tend to form a gel of needlelike aggregates. However, if the protons are also involved in such interactions, or trapped by such structures, then they are not available for conduction. Consequently, the effective number of charge carriers for S-PPTA will decrease. Under the same conditions, S-invert-PPTA also forms needlelike aggregates without gel formation. SEM analysis of these PPTA polymers showed quite different packing densities (Figure 4); S-PPTA appears to be far more compact that S-invert-PPTA. The slightly larger aggregate size and reduced affinity for water could account for the more dense structure that results upon drying. A more open, layered structure is certainly more apparent in the case of S-invert-PPTA and could provide another explanation for the improved conductivity of this material versus S-PPTA. The water uptake was also slighter lower in the case of S-PPTA, which is also expected to result in a slightly lower conductivity.

The sulfonated PPTA polymers are variants of the well-known rigid-rod polymer Twaron (also known as Kevlar). Through strong intermolecular interactions (hydrogen-bonding), PPTA forms liquid crystalline solutions in sulfuric acid that can subsequently be spun into high-strength fibers. This ability to form aligned structures in the solution state has also been retained by the sulfonated PPTA polymers, as demonstrated in previous publications from Viale et al.[26−31] Both S- and S-invert-PPTA exhibited a nematic liquid crystalline phase in water, at concentrations above 2 and 1 wt %, respectively, although liquid crystallinity, in the case of these sulfonated polymers, is a consequence of the formation of needlelike aggregates. The size of the aggregates varies between these two polymers, with S-PPTA displaying a slightly larger aggregate length and diameter. Films cast from those supramolecular liquid crystal solutions may exhibit a memory of the aggregation formation and orientation during drying process. The study of the film structure was investigated using wide-angle X-ray scattering (WAXS); the results are displayed below.

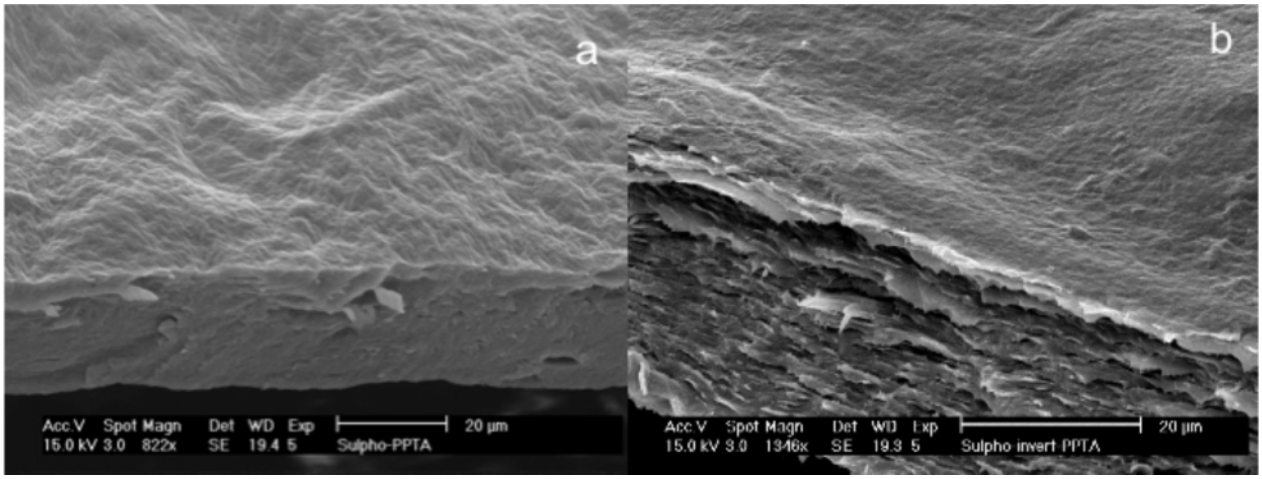

Figure 4. Scanning electron microscopy images of (a) S-PPTA and (b) S-invert-PPTA.

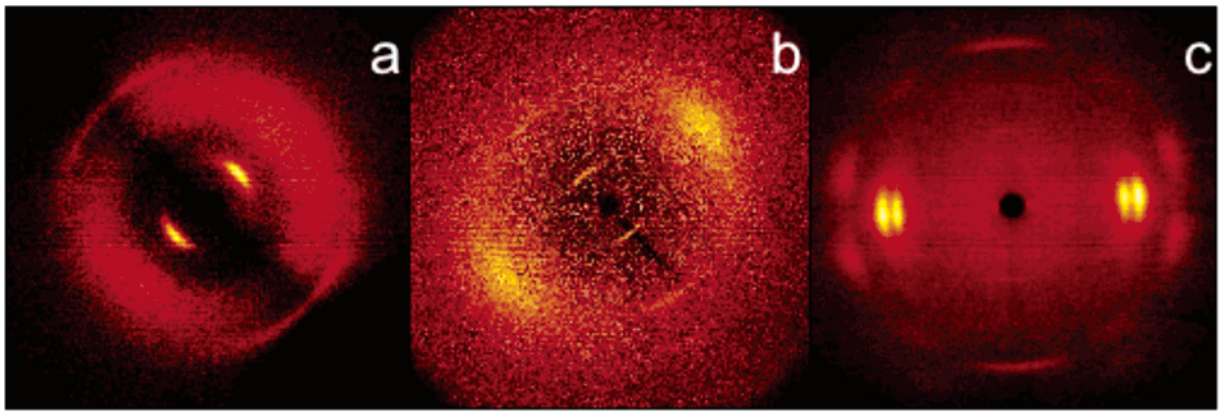

Figure 5. Wide-angle X-ray scattering images for (a) S-PPTA, (b) S-invert-PPTA, and (c) PPTA fiber. X-rays were incident in the plane of the sulfonated PPTA films and along the cross-section of the PPTA fiber.

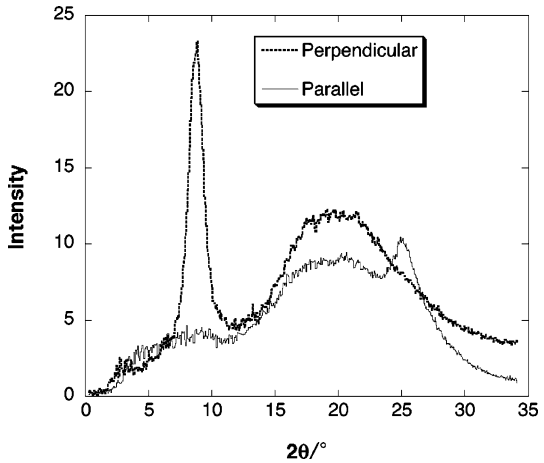

Figure 6. X-ray scattering intensity as a function of 2θ for S-PPTA in both the parallel and perpendicular directions.

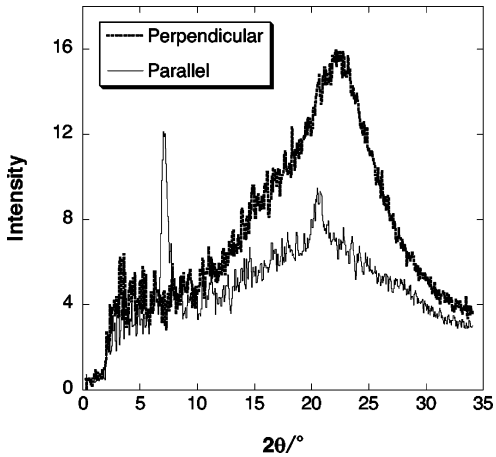

Figure 7. X-ray scattering intensity as a function of 2θ for S-invert-PPTA in both the parallel and perpendicular directions.

From X-ray diffraction of these polymers, anisotropic alignment was observed within the film, as seen from the scattering images in Figure 5. The incident X-rays were in the plane of the film, that is at a glancing angle to the film face. The scattering spots along the film direction—45° with the vertical—indicate a strong degree of alignment at the molecular level (Figure 5a and b). For comparison, Figure 5c displays the 2-D projection of the scattering of a PPTA fiber aligned along the vertical axis. It can easily be seen that in the case of the fiber, its (crystalline) structure is far more ordered than in the case of the sulfonated PPTA films. The known reflections for the PPTA fiber guide the following discussion of the sulfonated PPTA film structures.

The scattering intensities in parallel and perpendicular directions to the film (as displayed in Figure 5) were grouped in circular sectors in order to generate scattering intensities in those directions as a function of the scattering angle, 2θ. These results are displayed in Figures 6 and 7 for S-PPTA and S-invert-PPTA, respectively. Two curves are shown in each case corresponding to scattering perpendicular and parallel to the plane of the polymer film. For S-PPTA, scattering parallel to the film alignment resulted in a broad peak at about 19.4° and narrow peak of intermediate intensity at 25°, with the respective *d*-spacings being 4.6 and 3.6 Å. Scattering perpendicular to the film shows a strong narrow peak at 8.8° with a weaker broad peak observed at 19.5°, corresponding to *d*-spacings of 10.1 and 4.6 Å, respectively. For S-invert-PPTA, two parallel peaks were observed: a strong narrow peak at 7° (12.6 Å) and weaker narrow peak at 20.5° (4.3 Å). A single broad and quite weak perpendicular scattering peak was detected at 22.3° (4 Å).

With the sulfonated polymers being derivatives of PPTA, the molecular structures should exhibit some similarities, despite the absence of crystallinity in the present case. The X-ray diffraction of PPTA has been fully indexed[39,40] and the crystal structure is well defined. Table 3 lists the 2θ values and the related *d*-spacings corresponding to the diffraction planes of the PPTA lattice. The X-ray results for S-PPTA and S-invert-PPTA are also shown in this table. Comparing these values with the diffraction peaks for PPTA highlights the similarities between these polymers. All three polymers exhibit a peak at approximately 23°. Although quite strong and narrow in the case of the PPTA fiber, the peak is much weaker for the sulfonated polymers, with a very broad peak observed in the case of S-invert-PPTA. Another strong peak is observed for the PPTA fiber at approximately 20°. In S-PPTA, this peak is much weaker and very broad while for S-invert-PPTA, it appears to be masked by the diffraction peak at 23°. These peaks are probably related to interchain spacing and thus the broadness of these peaks for the sulfonated PPTA polymers suggests that the spacing is not well defined.

Another peak observed for all three polymers occurs at approximately 7° and arises from diffraction from the backbone of the polymer chain. In the case of the PPTA fiber, this peak is very weak and difficult to discern from the background.[39] For both the sulfonated PPTAs, however, the peak is very strong and narrow. The difference in intensity is related to the strongly diffracting sulfonic acid group. For the two sulfonated polymers, the *d*-spacings differ by about 2 Å: S-PPTA exhibits the smaller *d*-spacing. The gel behavior of S-PPTA in solution is probably the result of intermolecular interactions experienced by the

TABLE 3: X-ray Diffraction Peaks and *d*-Spacings for S-PPTA and S-Invert-PPTA[a]

S−PPTA		S-invert-PPTA		PPTA fiber[22,23]		
parallel		perpendicular		equatorial		
2θ	*d*-spacing	2θ	*d*-spacing	2θ	*d*-spacing	diffraction plane[b]
19.4°	4.6 Å			20.5°	4.3 Å	(110)
25°	3.6 Å	22.3°	4 Å	23°	3.9 Å	(200)
				28.2°	3.2 Å	(211)
perpendicular		parallel		meridional		
8.8°	10.1 Å	7°	12.6 Å	6.9°	12.8 Å	(001)
				13.7°	6.5 Å	(002)
19.5°	4.6 Å	20.5°	4.3 Å			
				27.1°	3.3 Å	(004)
				42.0°	2.2 Å	(006)

[a] Data for PPTA fiber shown for comparison, along with the corresponding diffraction planes.[39,40] [b] Diffraction planes for PPTA fiber only.

sulfonic acid group. It is possible that this interaction affects the polymer conformation within the film and, therefore, the resultant *d*-spacing. This will be discussed in more detail below.

For the PPTA fiber, diffraction is also detected at 2θ values of 13.7°, 27.1°, and 42° corresponding to intramonomer distances of 6.5, 3.3, and 2.2 Å respectively. While these same diffraction peaks were *not* observed for the sulfonated PPTA polymers, a peak at approximately 20° (4.4 Å) was detected instead. Again, the presence of the strongly diffracting sulfonic acid group probably enhances the signal intensity, allowing for this peak to be observed. For S-PPTA, the peak is very broad, while a small but narrow peak is observed on a broad background for S-invert-PPTA.

The degree of alignment was determined by fitting the intensity data as function of azimuthal angle, χ, with a Maier−Saupe type function[41] (eq 1).

$$I = I_0 + A \exp\{\alpha \cos^2(\chi - \chi_0)\} \quad (1)$$

In this equation, I is the scattering intensity, I_0 is the baseline scattering intensity, A is the amplitude of the scattering intensity, and α is the peak width. The distribution function of β (the angle of the director) is determined by substituting α into eq 2, which is then used obtain the average degree of alignment, $\overline{\langle P_2 \rangle}$ (eq 3). The order parameter values are 0.77 and 0.64 for S-PPTA and S-invert-PPTA, respectively.

$$f(\beta) = \exp(\alpha \cos^2 \beta) \quad (2)$$

$$\overline{\langle P_2 \rangle} = \frac{\int_{-1}^{1} f(\beta) P_2(\cos\beta) d\cos\beta}{\int_{-1}^{1} f(\beta) d\cos\beta} \quad (3)$$

The higher molecular weight of S-PPTA (see Table 1) could favor a higher degree of alignment, thus accounting for the difference in the $\overline{\langle P_2 \rangle}$ values. However, intermolecular interactions are also more dominant in the case of S-PPTA, and could assist in the aggregate alignment. It is quite likely that experimental conditions such as film drying speed, final film thickness, etc. also influence the aggregate interactions, and thus the resultant ordering of the polymer chains within the film.

Although similar peak positions were observed for both sulfonated PPTA polymers, the orientation of these peaks is *rotated* with respect to one another, i.e., the scattering peaks that are perpendicular to the plane of the S-PPTA film are parallel to the film for S-invert-PPTA. Consequently, S-PPTA molecules appear to align homeotropically (perpendicular to the film plane), while S-invert-PPTA exhibits a random planar alignment of nematic domains. Given that the two polymers are chemically identical, it was expected that the film microstructures should also be similar. Furthermore, previous scattering studies showed that the dimensions of the aggregates are very similar in both systems prepared under the same conditions and concentration, typically exhibiting a cross-section of a few nanometers and a length approaching a micrometer.[26,27] Therefore, there must be other factors during film formation that influence the resultant structure.

Water solutions of these polymers presented very different properties, with S-PPTA forming a nematic *gel* of needlelike aggregates at low concentrations, while S-invert-PPTA is a free flowing nematic *solution* of needlelike aggregates. It is likely that the absence or presence of the gel in solution will strongly affect the resultant molecular orientation in the dried film. During the drying process, it is speculated that three types of interactions may be present: the aggregate-aggregate interaction that drives the nematic order and changes with increasing concentration during drying,[42] the aggregate interaction with the substrate that tends to align the aggregates parallel to the plane of the film, and the upward flow of evaporating solvent that opposes the substrate interaction and tends to align the nematic aggregates, and the molecules therein, homeotropically. The rate of water evaporation is also an important factor as this governs the time during which aggregate reorientation can occur. It was previously shown that the characteristic rotation time for the S-PPTA aggregates was around 30 h for a 1 wt % solution.[29] In contrast, the relaxation time in a 6 wt % solution of S-invert-PPTA was about 2.5 h.[28] Logically, the relaxation times should be even faster for more dilute solutions of S-invert-PPTA. It is, therefore, hypothesized that the balance of aggregate−aggregate and aggregate−substrate interactions in combination with the characteristic rotation times should account for the final molecular orientation in the dried film.

SEM analysis of the film structures (Figure 4) also appears to support the above hypothesis. S-invert-PPTA exhibits an open layered structure parallel to the plane of the film and is consistent with the planar alignment of the polymer chains that was observed from the X-ray scattering. On the other hand, the SEM image of S-PPTA shows a very compact structure from which it is difficult to discern definitive layering. Close inspection, however, does reveal a tendency for a more vertical texturing through the cross-section of the film, as would be expected for a homeotropically aligned polymer. It is important to recognize the impact of the polymer alignment on the other film properties, in particular the proton conductivity. As the conductivity measurements were conducted in the plane of the film, it is expected that proton transport should be more efficient in polymer with planar alignment. Indeed, the evidence supports this, with planar aligned S-invert-PPTA exhibiting proton

conductivities that are at least two times higher than the homeotropically aligned S-PPTA in that direction. Unfortunately, it has not been possible to confirm this conclusion with the analogous measurement through the thickness of the film. These results, however, have important implications on the designing of polymer membranes for fuel cell applications.

4. Conclusions

A series of sulfonated poly(*p*-phenylene terephthalamide) (PPTA) polymers are considered for new fuel cell membrane materials. The rigid-rod nature of the polymers provides both mechanical and thermal stability, while the high degree of sulfonation (at least 3 times that of Nafion) should allow for exceptional proton conductivities. The properties, however, are sensitive to the position of the sulfonic acid group. S-PPTA forms a gel in water and the films also take up less water than the counterpart, S-invert-PPTA. Conductivities for both polymer films are comparable to Nafion, with S-invert-PPTA demonstrating slightly higher values. However, when taking into consideration the higher charge carrier concentration for the sulfonated PPTAs, it is apparent that the mobility must be restricted by the polymer film structure. Structure analysis by X-ray diffraction indicated that both molecules are aligned in the films. The direction of the alignment, however, was different for each; S-PPTA was aligned homeotropically while S-invert-PPTA was aligned in the plane of the film. SEM analysis supported these findings, with evidence of layering on the microscopic scale in the same direction as the polymer chain alignment. The resultant film structure appears to be strongly dependent on the solution properties. The alignment is also expected to have implications on the proton conductivity, which is currently under further investigation.

Acknowledgment. This research forms part of the research program of the Dutch Polymer Institute (DPI), project #457.

References and Notes

(1) Vallejo, E.; Pourcelly, G.; Gavach, C.; Mercier, R.; Pineri, M. *J. Membr. Sci.* **1999**, *160*, 127.
(2) Cornet, N.; Diat, O.; Gebel, G.; Jousse, F.; Marsacq, D.; Mercier, R.; Pineri, M. *J. New Mater. Electrochem. Syst.* **2000**, *3*, 33.
(3) Cornet, N.; Beaudoing, G.; Gebel, G. *Sep. Purif. Technol.* **2001**, *22*−*23*, 681.
(4) Genies, C.; Mercier, R.; Sillion, B.; Petiaud, R.; Cornet, N.; Gebel, G.; Pineri, M. *Polymer* **2001**, *42*, 5097.
(5) Blachot, J. F.; Diat, O.; Putaux, J.-L.; Rollet, A.-L.; Rubatat, L.; Vallois, C.; Müller, M.; Gebel, G. *J. Membr. Sci.* **2003**, *214*, 31.
(6) Einsla, B. R.; Hong, Y.-T.; Kim, Y. S.; Wang, F.; Gunduz, N.; McGrath, J. E. *J. Polym. Sci., Part A: Polym. Chem.* **2004**, *42*, 862.
(7) Einsla, B. R.; Kim, Y. S.; Hickner, M. A.; Hong, Y.-T.; Hill, M. L.; Pivovar, B. S.; McGrath, J. E. *J. Membr. Sci.* **2005**, *255*, 141.
(8) Kobayashi, T.; Rikukawa, M.; Sanui, K.; Ogata, N. *Solid State Ionics* **1998**, *106*, 219.
(9) Kopitzke, R. W.; Linkous, C. A.; Anderson, H. R.; Nelson, G. L. *J. Electrochem. Soc.* **2000**, *147*, 1677.
(10) Jones D. J.; Rozière, J. *J. Membr. Sci.* **2001**, *185*, 41.
(11) Xing, P.; Robertson, G. P.; Guiver, M. D.; Mikhailenko, S. D.; Wang, K.; Kaliaguine, S. *J. Membr. Sci.* **2004**, *229*, 95.
(12) Kaliaguine, S.; Mikhailenko, S. D.; Wang, K. P.; Xing, P.; Robertson, G.; Guiver, M. *Catal. Today* **2003**, *82*, 213.
(13) Wang, F.; Chen T.; Xu, J. *Macromol. Chem. Phys.* **1998**, *199*, 1421.
(14) Wang, F.; Chen, T.; Xu, J. *Macromol. Rapid. Commun.* **1998**, *19*, 135.
(15) Xiao, G.; Sun, G.; Yan, D. *Polym. Bull.* **2002**, *48*, 309.
(16) Wang, F.; Hickner, M.; Ji, Q.; Harrison, W.; Mecham, J.; Zawodzinski, T. A.; McGrath, J. E. *Macromol. Symp.* **2001**, *175*, 387.
(17) Wang, F.; Hickner, M.; Kim, Y. S.; Zawodzinski, T. A.; McGrath, J. E. *J. Membr. Sci.* **2002**, *197*, 231.
(18) Kim, Y. S.; Wang, F.; Hickner, M.; McCartney, S.; Hong, Y. T.; Harrison, W.; Zawodzinski, T. A.; McGrath, J. E. *J. Polym. Sci., Part B: Polym. Phys.* **2003**, *41*, 2816.
(19) Kim, Y. S.; Dong, L.; Hickner, M. A.; Pivovar, B. S.; McGrath, J. E. *Polymer* **2003**, *44*, 5729.
(20) Kim, Y. S.; Hickner, M. A.; Dong, L.; Pivovar, B. S.; McGrath, J. E. *J. Membr. Sci.* **2004**, *243*, 317.
(21) Hickner, M. A.; Ghassemi, H.; Kim, Y. S.; Einsla, B. R.; McGrath, J. E. *Chem. Rev.* **2004**, *104*, 4587.
(22) Harrison, W. L.; Hickner, M. A.; Kim Y. S.; McGrath, J. E. *Fuel Cells* **2005**, *5*, 201.
(23) Taeger, A.; Vogel, C.; Lehmann, D.; Jehnichen, D.; Komber, H.; Meier-Haack, J.; Ochoa, N. A.; Nunes, S. P.; Peinemann K.-V. *React. Funct. Polym.* **2003**, *57*, 77.
(24) Meier-Haack, J.; Taeger, A.; Vogel, C.; Schlenstedt, K.; Lenk W.; Lehmann, D. *Sep. Purif. Technol.* **2005**, *41*, 207.
(25) Vogel, C.; Meier-Haack, J.; Taeger A.; Lehmann D. *Fuel Cells* **2004**, *4*, 320.
(26) Viale, S.; Best, A. S.; Mendes, E.; Jager W. F.; Picken, S. J. *Chem. Commun.* **2004**, 1596.
(27) Viale, S.; Mendes, E.; Picken S. J.; Santin O. *Mol. Cryst. Liq. Cryst.* **2004**, *411*, 525.
(28) Viale, S.; Mendes E.; Picken, S. J. *Mol. Cryst. Liq. Cryst.* **2005**, *437*, 43.
(29) Mendes, E.; Viale, S.; Santin, O.; Heinrich M.; Picken S. J. *J. Appl. Cryst.* **2003**, *36*, 1000.
(30) Viale, S.; Jager, W. F.; Picken, S. J. *Polymer* **2003**, *44*, 7843.
(31) Viale, S.; Li, N.; Schotman, A. H. M.; Best, A. S.; Picken S. J. *Macromolecules* **2005**, *38*, 3647.
(32) Viale, S.; Best, A. S.; Mendes E.; Picken S. J. *Chem. Commun.* **2005**, 1528.
(33) Gibbard, Jr., H. F.; Scatchard, G. *J. Chem. Eng. Data.* **1973**, *18*, 293.
(34) Zawodzinski, Jr., T. A.; Springer, T. E.; Davey, J.; Jestel, R.; Lopez, C.; Valerio J.; Gottesfeld, S. *J. Electrochem. Soc.* **1993**, *140*, 1981.
(35) Grozema, F. C.; Best, A. S.; van Eijck, L.; Stride, J.; Kearley, G. J.; de Leeuw, S. W.; Picken, S. J. *J. Phys. Chem. B.* **2005**, *109*, 7705.
(36) Rieke P. C.; Vanderborgh, N. E. *J. Membr. Sci.* **1987**, *32*, 313.
(37) Oberbroeckling, K. J.; Dunwoody, D. C.; Minteer, S. D.; Leddy, J. *Anal. Chem.* **2002**, *74*, 4794.
(38) Yang, H. H. *Kevlar Aramid Fiber*; John Wiley & Sons Ltd: West Sussex, 1993.
(39) Northolt, M. G. *Eur. Polym. J.* **1974**, *10*, 799.
(40) Panar, M.; Avakian, P.; Blume, R. C.; Gardner, K. H.; Gierke, T. D.; Yang, H. H. *J. Polym. Sci., Part B: Polym. Phys.* **1983**, *21*, 1955.
(41) Picken, S. J.; Aerts, J.; Visser, R.; Northolt, M. G. *Macromolecules* **1990**, *23*, 3849.
(42) Onsager, L. *Annu. NY Acad. Sci.* **1949**, *51*, 627.